Accident Analysis of Heat Pipe Cooled Space Reactor

Yuan Yuan, Jianqiang Shan, Bin Zhang*, Junli Gou, Bo Zhang
School of Nuclear Science and Technology, Xian Jiaotong University
No.28, Xianning West Road, Xi'an, Shaanxi, 710049, P.R. China

ABSTRACT

A space power with high power density, light weight, low cost and high reliability is of crucial importance to future exploration of deep space. Space reactor is an excellent candidate because of its unique characteristics of high specific power, low cost, strong environment adaptability and so on. Among all types of space reactors, heat pipe cooled space reactor, which adopts the passive heat pipe as core cooling component, is considered as one of the most promising choice and is widely studied all over the world.

A transient analysis code (TAPIRS) for heat pipe cooled space reactor power system is developed. The TAPIRS based on point reactor kinetics model, lumped parameter core heat transfer model, combined heat pipe (HP) model (self-diffusion model, flat-front startup model and network model), energy conversion model of alkali metal thermal-to-electric conversion units (AMTEC), and HP radiator model. Three typical accidents, i.e., control drum failure, AMTEC failure and partial loss of the heat transfer area of radiator are then analyzed using TAPIRS. The results show that the heat pipe cooled space reactor has excellent inherent safety characteristics.

Key Words: Space reactor; Heat pipe; AMTEC; Accident

1 INTRODUCTION

In the design of space reactor, accident analysis plays an important role. However, published accident analysis is still not so much, while the published ones are usually focusing on the accidents in liquid metal cooled space reactors, not heap pipes cooled ones. Poston et. al.[1] analyzed the failed heat pipe scenarios showed that the temperatures in modules that do not touch the failed module are unaffected. El-Genk et. al.[2] analyzed the system transient responses induced by the change of the system load in alkali metals cooled ScoRe-TE. Poston et. al.[3] developed a FRINK code to perform the transient analysis after a continuous reactivity insertion in a simplified reactor system. Shannon M and James [4]introduced a reactivity control method by control drum in space reactors. Jeffrey C et. al.[5] analyzed launch failure accidents in space reactor. Adam R and Andrew C[6] designed and constructed a new electric heating device to simulate the reactor system under the transient conditions. Bushman et. al.[7] designed a new 100kWe space reactor system and described the main components in detail on the comprehensive consideration of structure and material. Ran et. al.[8] perform transient thermal hydraulics analysis of a 200kW advanced space fast reactor RAPID-L on reactor life, startup characteristics and transient performance under UTOP and ULOF.

Accident analysis under different space reactor accidents is essential to the development of the space reactor. This paper chooses typical heat pipe cooled space reactor, SAIRS (Scalable AMTEC Integrated R eactor Space Power Systems), as research object and performs accident analysis under three typical accid ents of control drum failure, AMTEC failure, and partial loss of heat transfer area of radiator after system atic modeling of its each module.

* Corresponding author. Tel.: +86 029 82663769; fax: +86 029 82663769
E-mail address: binzhang@xjtu.edu.cn

2 SYSTEM DESCRIPTION

El-Genk and Tournier[10] presented their design for the SAIRS power system. In this system a fast neutron spectrum nuclear reactor is cooled with a Na-HPs, and 18×5.6kWe Na-AMTEC units. The AMTEC units are divided into six blocks of 3 units and each block is cooled by K-HPs in a separate radiator panel. The AMTEC units, placed behind the radiation shadow shield, are heated by sodium HPs. The six AMTEC blocks in the power system are connected electrically in parallel. SAIRS has a nominal electrical power of 110kWe that is delivered at a terminal voltage of 400 V DC. The SAIRS HP-cooled nuclear reactor is comprised of 60 fuel modules. Each fuel module consists of three uranium nitride (UN), rhenium (Re) clad fuel pins arranged in a triangular lattice. Figure 1 shows the schematic diagram of this space reactor.

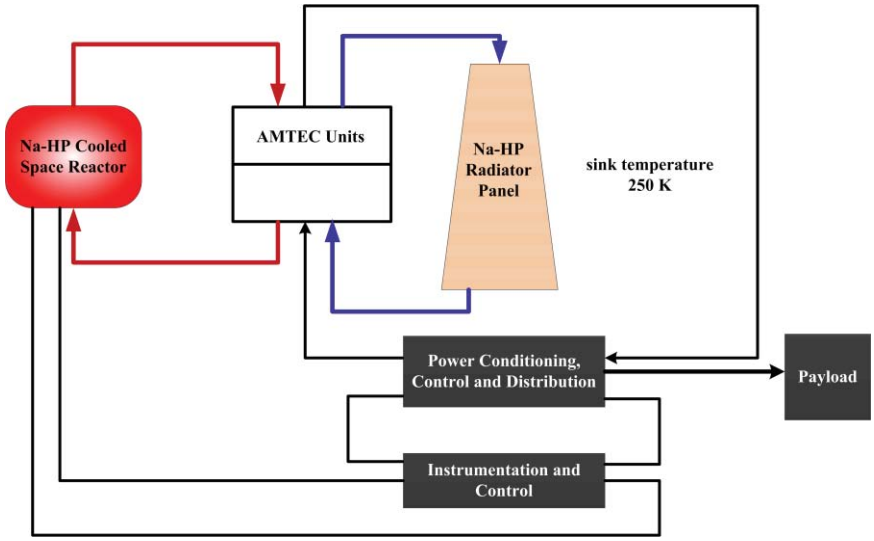

Figure 1 Schematic figure of primary and secondary HP loops of HPS

Point reactor kinetics model: The standard point reactor kinetics equations with six delayed neutron groups are solved to determine the reactor power given a specified input reactivity. The total reactivity is determined by including the core average temperature feedback effect[9].The end floating method with hi gh-order polynomial approximation [10] for solving the point reactor neutron kinetics equations.

Core heat transfer model: The cladding along the active length of the fuel pins in SAIRS is brazed to a central Mo-14%Re/Na-HP, as shown in Figure 2. For the convenience of calculating heat transfer between HP and the fuel pins, the triangle region is simplified as an annular layer surrounding the clad, and its thickness is calculated based on the triangle area. Therefore, the fuel rod is composed of four layers: fuel pellets, gap, clad and imagined outer layer respectively. Lumped-parameter models [11] can be used for the prediction of transient conduction in nuclear reactor components because of UN fuel's good heat transfer characteristics. Different from Wulff's model[11], the governing equation of imagined outer layer should be added. The process of transient, axisymmetric radial conduction through the fuel pellet, gap, concentric clad and imagined outer layer is shown in Figure 2. Fourth-Order Runge–Kutta scheme is used to solve the fuel temperature differential equations.

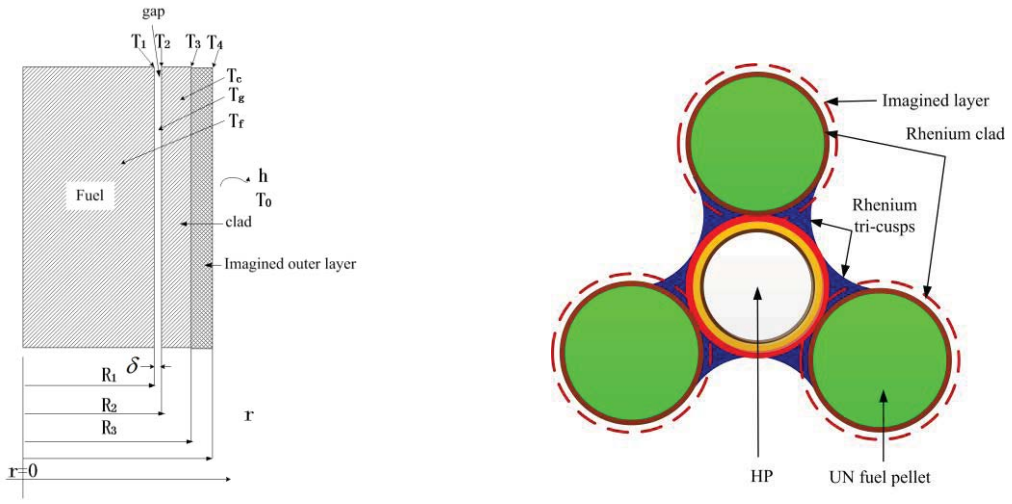

Figure 2 Geometry for fuel element

Combined HP model: HP usually consists of wall, porous wick, and vapor core. In order to reduce the circulation pressure drop, the space reactor adds a liquid annulus, as shown in Figure 3. Therefore, the wick is separated from the wall by an annulus filled with working liquid. The startup process of a liquid metal HP from the frozen state may be divided into several phases for the convenience of analysis. Enormous work has been devoted on the mathematical formulation of every HP Phase. This paper incorporates them into one model based on these mature models, as shown in Table 1.

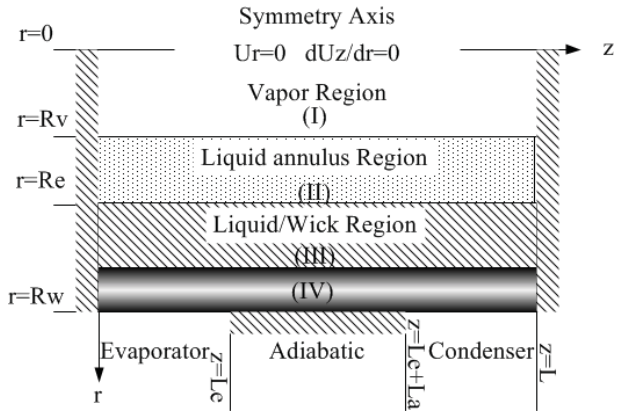

Figure 3 HP physical model and boundary conditions

Table 1 The HP models

Model	Startup Phases	References
The self-diffusion model	1-3	Ochterbeck J(1997)[12]
The flat-front startup model	4	Y.Cao(1993)[13]
The “network” model	5	ZUO(1998)[14]

Figure 4 illustrates the network of the heat transfer between the evaporator and the condenser. The existence liquid annulus makes the modeling of the HP adopted here unique. Because of adding a liquid annulus, the network model adds three thermal resistances which are evaporator liquid annulus radial direction thermal-conduction resistance (2 in Figure 4), adiabatic liquid annulus radial direction thermal-conduction resistance (6 in Figure 4) and condenser liquid annulus radial direction thermal-conduction resistance (10 in Figure 4). The mathematical formulation of the HP modeling should make the change correspondingly.

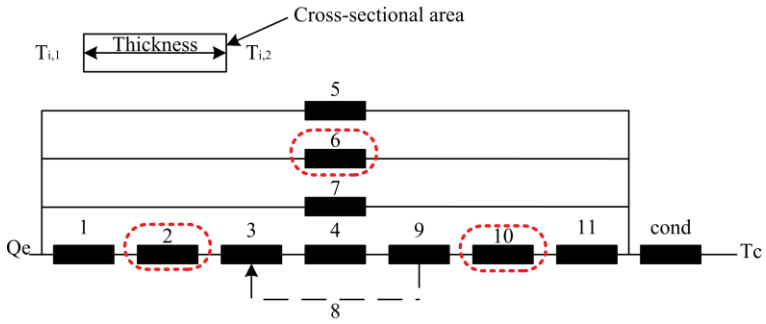

Q_e-Evaporator heat input;1-Evaporator wall (radial direction); *2-Evaporator liquid annulus (radial direction)*; 3-Evaporator wick (radial direction); 4-Vapor flow (heat convection); 5-Adiabatic wick (axial direction); *6-Adiabatic liquid annulus (radial direction)*; 7-Adiabatic wall (axial direction); 9-Condenser wick (radial direction); *10-Condenser liquid annulus (radial direction)*;11-Condenser wall (radial direction); Cond-Convective cooling condition (condenser outer surface).

Figure 4 A one-dimensional heat conductor

For the alkali metal high temperature HP, seven heat transfer limitations should be considered. Five of them are physical factors limiting the heat flux in HP: the viscous limit, the sonic velocity limit, the entrainment limit, the boiling limit and the capillary limit. There are four limits include frozen startup limit, viscous limit, continuous flow limit and sonic limit must considered in the startup condition [7].

AMTEC model: Tournier [15] conducted a number of AMTEC design studies and steady-state analysis. The high performance AMTEC Model consists of four, interactively coupled sub-models: (a) Pressure loss model; (b) Electrochemical model; (c) Electrical model; (d) Thermal model. For the transient analysis of the AMTEC, the components temperature, working fluid flow rate, and heat transfer should be coupled. In this paper we add the transient temperature equation to calculate the evaporator and condenser temperature in AMTEC.

Radiator model: Each radiator panel has two sections that are thermally coupled using six, double vapor cavity K-HP. Lumped-parameter models can be used for the prediction of transient conduction in radiator panel.

Because of the lake of papers and codes which are analyze HPS accidents, the whole system accidents have not been validated, but the component models has been validated with the references. The point reactor kinetics model was compared with Yuan and Hu[10], the lumped parameter core heat transfer model was compared with Wuff[11], the combined HP model was compared with El-Genk etc.[12-14] and the energy conversion model for AMTEC was compared with El-Genk etc.[16]. The specific validation work can be seen in the report[17].

3 ACCIDENT ANALYSIS

3.1 Control Drum Failure

The simulated nominal steady-state operation parameter is assumed the system generates 110kWe at the condition of 60VDC and reactor exit temperature of 1202K. Thermal power is 400 kWth and overall system efficiency is around 27%. The Na-HP in the core and K-HP in the radiator is 1189K and 680K respectively. The nominal temperature across the AMTEC is 1169 and 700K, respectively.

A thin shutter B4C occupies a portion of the face of the drum. This material absorbs neutrons and provides reactor control. With all drums rotated in toward the core, the beginning of life (BOL) the reactor core has an excess reactivity of $2.12, and with the drums in their minimum worth position, the

excess reactivity would be -$9.52. Worth is a function of both the poison distance from the core and the angular fraction of the core occluded and uncontrolled rotation of control drum will cause an insertion of reactivity.

This section presents the results on the response of the HPS to a control drum failure from a nominal steady-state. The HPS arranges two sets of control drums. In this paper we assume only one set of control drums fail. In the accident the B4C segments in the control drums placed in the radial BeO reflector face 180° away from the reactor core and the HPS reactor core has an excess reactivity of $1.43 (point 2 in Figure 5). Melting temperature of UN fuel and rhenium is ~ 2630℃and 3180℃,respectively.

The BeO/B4C drums rotate outward at an angular speed of 0.03°/s after 50s steady-state operation. This accident ends at 8000s later, when the total external reactivity insertion reaches $1.43. At that time, the total reactivity is positive and the external reactivity is larger than the reactivity feedback (Figure 5), so the reactor thermal power increases (Figure 6). With the increase of the reactor temperature (Figure 7), the negative reactivity feedback will also increase, which will mitigate the power increase. The first reactor thermal power peak appears around 1000s.

Around 8000s in the failure transient, the control drums face 180° away from the reactor core, and external reactivity insertion stops. The reactor thermal power peaks at ~950kWth (Figure 6). Also, the temperatures of Na-HP in the core and K-HP in the radiator are ~2100K and ~850K, respectively (Figure 7 and Figure 8). The corresponding nominal steady-state temperature of the HP exiting the reactor core is 1200K. The open-circuit voltage of the system is ~400V at the beginning and ~780V after 8000s. The electrical power eventually reaches a nominal steady state value of ~320kW (Figure 12). The net conversion efficiency of the system increases from 27% initially to 34% (a 26% rise, Figure 10) and the reactor thermal power increases from its nominal value of 400 kWth to 950 kWth (a 137% increase, Figure 6).

The AMTEC efficiency is large than the nominal operation value. Increasing AMTEC evaporator temperature causes efficiency to increase due to the sharp rise in the vapor pressure of the alkali metal working fluid in the high pressure side of the AMTEC units. Such rise in the vapor pressure also increases the electrochemical potential generated across the BASE and hence, the electrical power output of the AMTEC units. The increase rejection heat means also an increase in the radiator panel temperature.

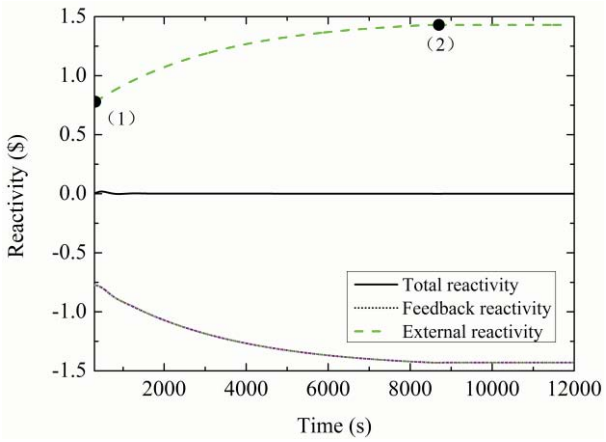

Figure 5 Reactivity variation during control drum failure

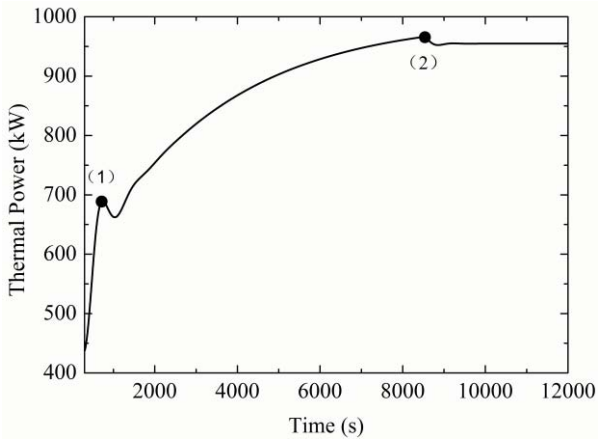

Figure 6 Calculated thermal power temporal profile during control drum failure

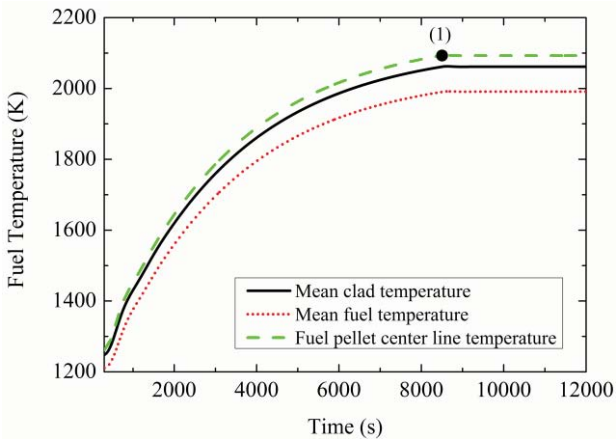

Figure 7 Calculated fuel temperature temporal profile during control drum failure

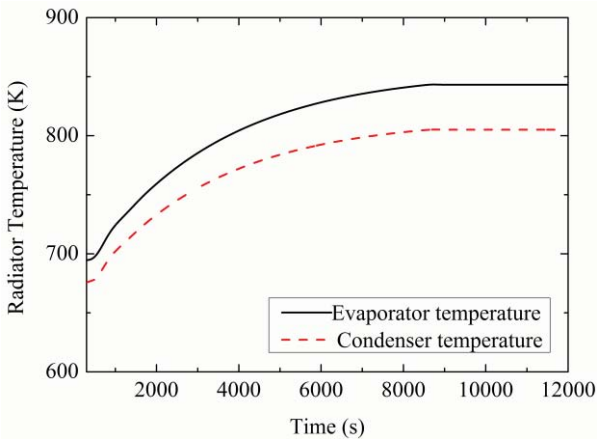

Figure 8 Calculated radiator temperature temporal profile during control drum failure

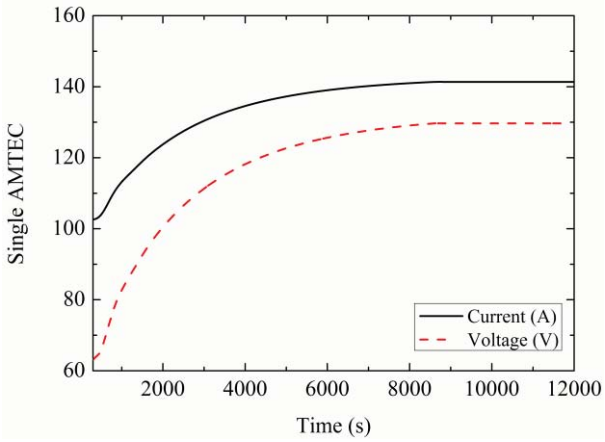

Figure 9 Calculated AMTEC current and voltage temporal profile during control drum failure

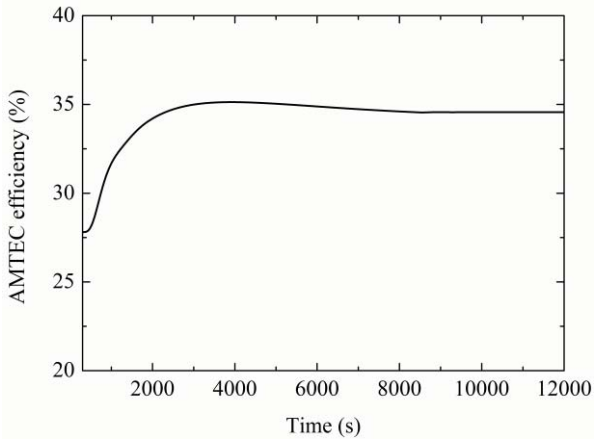

Figure 10 Calculated AMTEC efficiency temporal profile during control drum failure

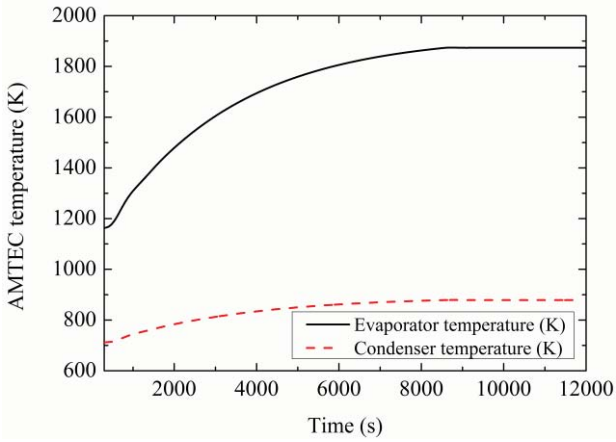

Figure 11 Calculated AMTEC temperature temporal profile during control drum failure

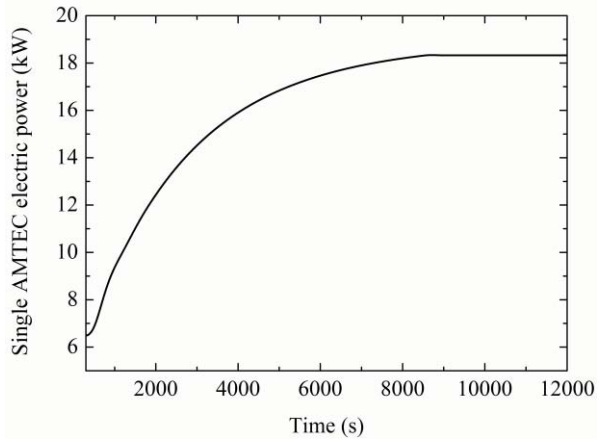

Figure 12 Calculated AMTEC electric power temporal profile during control drum failure

3.2 AMTEC Failure

In this accident, one AMTEC element fails suddenly after reactor steadily operates for 50s. Under this condition, other operational conditions are unchanged except that the AMTEC elements serially connected with the failed one cannot transfer electricity to the load. Finally, the electric power of these AMTECs converts into the heat emitted from the radiators. This is the reason of the increase of the heat transfer from single K heat pipe (Figure 13) and the increase of the temperature of radiators (Figure 14). This also results in the increase of the AMTEC cold junction which is connected with the radiators. Accordingly, the pressure difference between the two sides (high and low) of AMTEC will decrease, which will directly decrease the electricity voltage of AMTEC (Figure 16). As shown in Figure 15, the efficiency of AMTEC reduces to below 20%, which demonstrates that the electricity voltage and power of AMTEC are sensitive to the pressure difference between the high pressure and low pressure cavities. After the accident is initiated at 50s, other systematic parameters reach to their stable values except the reactor power, which stabilizes around 1500s after the accident. According to the calculation of TAPIRS, the temperature of the hot junction of radiators reaches to around 850K, while the heat transfer from K heat pipes stabilizes around 9kW, which is below the limit of heat pipe (18kW). The K heat pipe is concluded to be safe based on the fact of the heat transfer from heat pipes combined with the facts that the calculated temperatures of heat pipes are below their corresponding limits (2617.0℃ for Molybdenum, 1650℃ for Carbon-Carbon composite).

If the input heat to AMTEC remains constant, the increase of the cold junction of AMTEC will reduce the efficiency of AMTEC, pressure difference between the high pressure and low pressure cavities, and the temperature difference between the hot end and cold end of AMTEC. This can, to some extent, compensate for the increase of the hot end temperature (Figure 17). This shows that SAIRS is a space electric power system with flexible capability. The heat removal capability can be intensified by increasing the temperature of radiators. The induced temperature variation can be mitigated by the change of AMTEC efficiency.

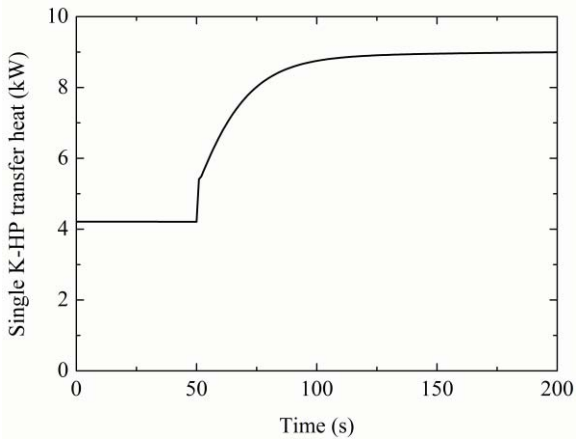

Figure 13 Calculated single K-HP transfer heat temporal profile during AMTEC failure

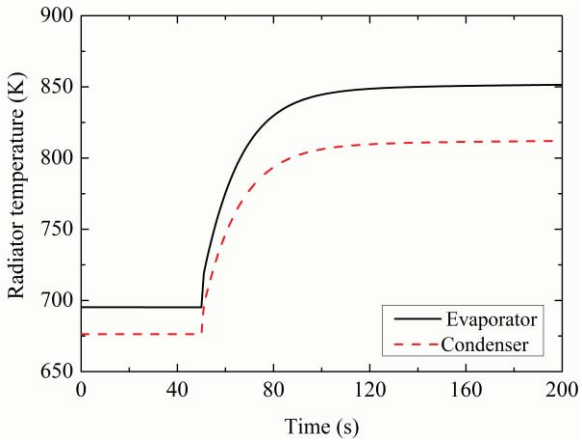

Figure 14 Calculated radiator temperature temporal profile during AMTEC failure

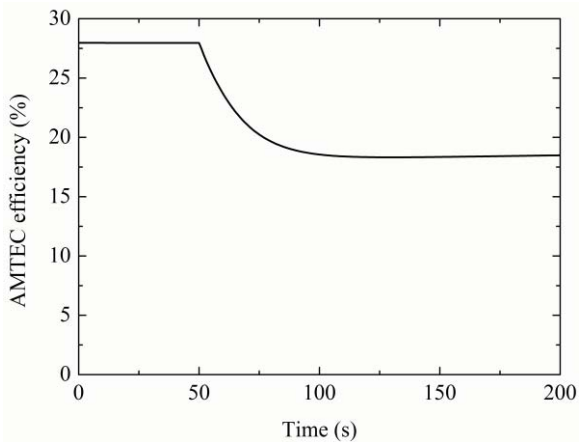

Figure 15 Calculated AMTEC efficiency temporal profile during AMTEC failure

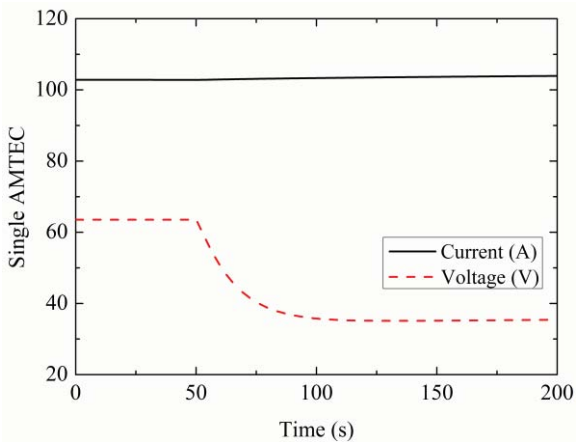

Figure 16 Calculated AMTEC current and voltage temporal profile during AMTEC failure

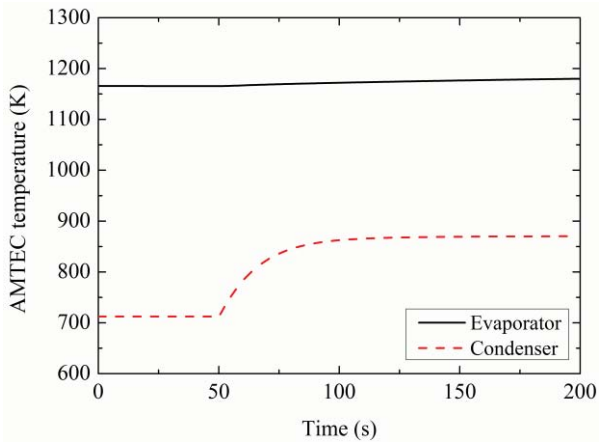

Figure 17 Calculated AMTEC temperature temporal profile during AMTEC failure

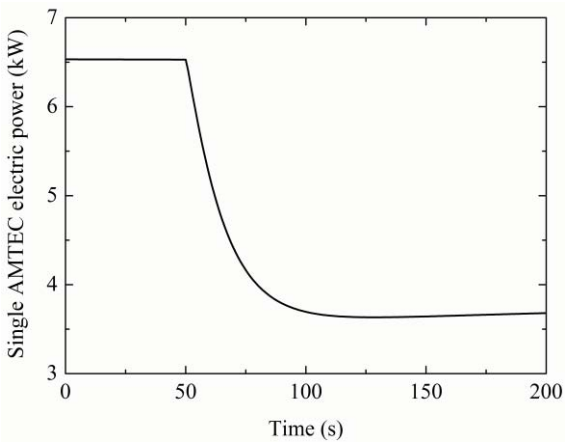

Figure 18 Calculated single AMTEC electric power temporal profile during AMTEC failure

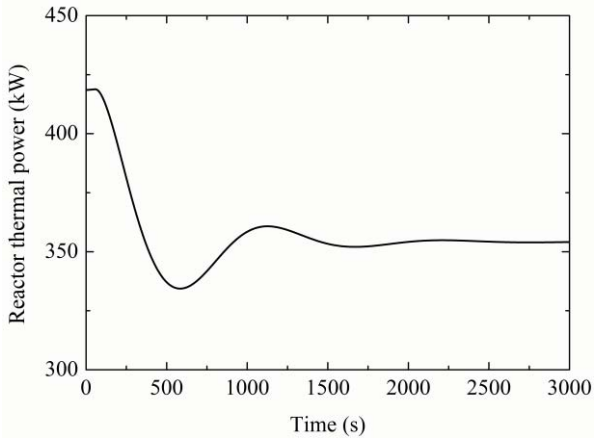

Figure 19 Calculated thermal power temporal profile during AMTEC failure

3.3 Partial Loss of the Heat Transfer Area

In this accident, the heat transfer area at the cold end of radiator heat pipes loses half of them after 10s' normal operation. Similar with the AMTEC failure accident, this accident will cause the increase of radiator temperature. To compensate for the partial loss of the heat transfer area of radiator, the surface temperature of radiator will increase to guarantee the heat removal. The radiator is made up of two-steam -cavity K heat pipes. The cold end is connected with the condensation section of K heat pipes, while the hot end contacts the evaporation section. The temperature increase of the radiator cold end will increase the temperature of cold end of K heat pipe by conduction (Figure 21), thus reduce the temperature difference between the evaporation section and condensation section of heat pipe. This is the reason of the reduction of heat transfer in K heat pipe (Figure 20). Finally the temperature of the evaporation section of K heat pipe is around 750K (Figure 21). The temperature of AMTEC cold end will also increase because it directly contacts the evaporation section of K heat pipe, which reduce the pressure difference between the high pressure and low pressure cavity of AMTEC, the output electricity voltage, and the efficiency of AMTEC (to around 25%, Figure 23). Finally, the reactor reaches to a steady state under the feedback of temperature. The heat pipes is safe based on the fact that the calculated heat transfer (4kW) in K heat pipe is still below its limit (15kW). The heat pipes work under the acceptable safe range.

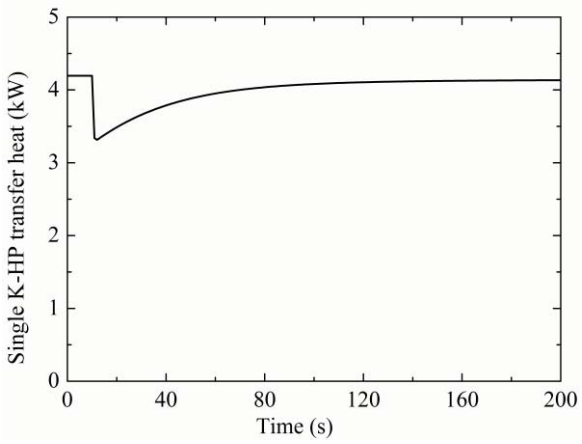

Figure 20 Calculated single K-HP transfer heat temporal profile during radiator failure

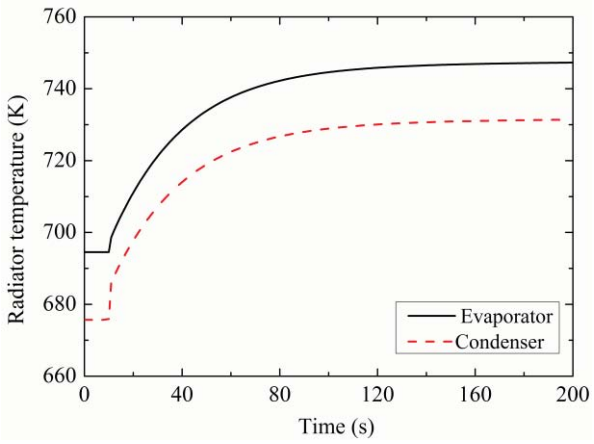

Figure 21 Calculated radiator temperature temporal profile during radiator failure

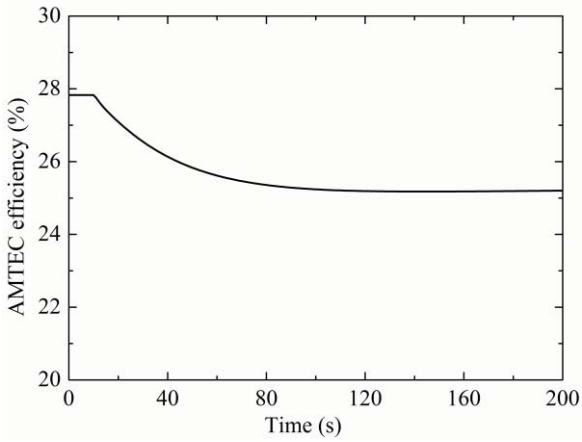

Figure 22 Calculated AMTEC efficiency temporal profile during radiator failure

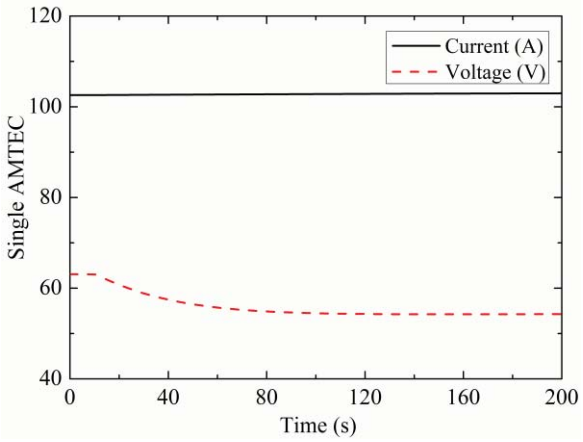

Figure 23 Calculated AMTEC current and voltage temporal profile during radiator failure

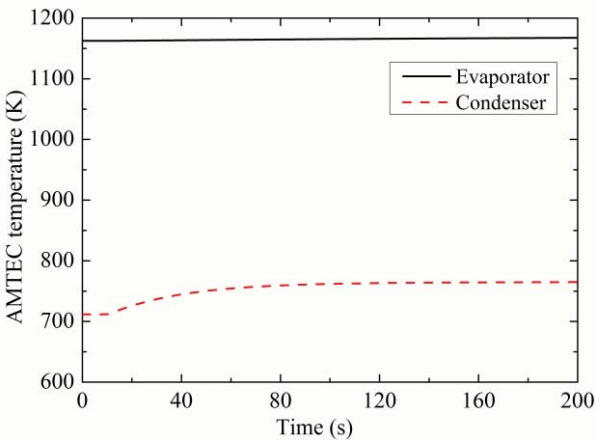

Figure 24 Calculated AMTEC temperature temporal profile during radiator failure

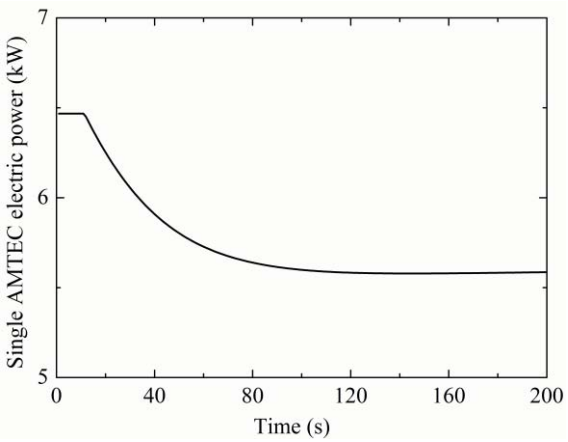

Figure 25 Calculated single AMTEC electric power temporal profile radiator radiator failure

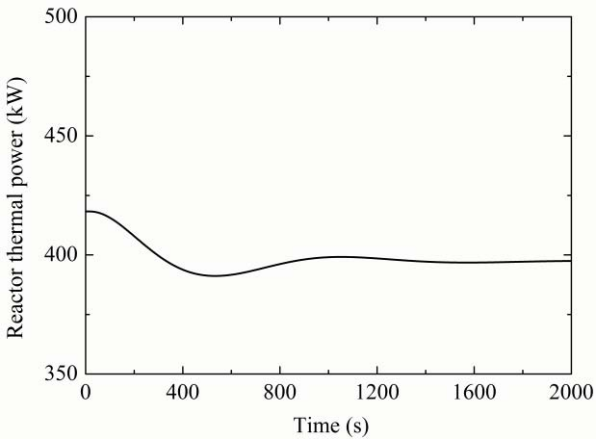

Figure 26 Calculated thermal power temporal profile during radiator failure

4 CONCLUSION

This paper introduces a system code (TAPIRS) capable of modeling the HPS. Three typical accidents, i.e., control drum failure, AMTEC failure and partial loss of the heat transfer area of radiator, is analyzed by TAPIRS. Comprehensive evaluation on reactor power, fuel temperature, AMTEC temperature, radiator temperature, AMTEC efficiency, and the temporal variation of current and electric voltage of AMTEC shows that the reactor remains safe under all these three typical accidents.The results show that: (1) After the failure of one control drum, the reactor power finally reaches to a stable value after two local peaks under the temperature feedback. The fuel temperature rises rapidly, however it is still under safe limit. (2) The fuel temperature is under safe limit under the AMTEC failure and partial loss of the heat transfer area of radiator. This demonstrates the rationality of the system design and the potential applicability of the TAPIRS code for the future engineering application of heat pipe cooled space reactor.

5 REFERENCES

1. Poston, D.I., R.J. Kapernick, and R.M. Guffee, *Design and analysis of the SAFE-400 space fission reactor*, 2002. p. 578-588.
2. El-Genk, M.S., *DynMo-TE: Dynamic Simulation Model of Space Reactor Power System with Thermoelectric Converters.* Nuclear engineering and design, 2006. **236**(23): p. 2501-2529.

3. Poston, D.I., et al., *FRINK — A Code to Evaluate Space Reactor Transients.* 2007. **880**: p. 449-457.
4. Bragg-Sitton and S. M., *Reactor Start-up and Control Methodologies: Consideration of the Space Radiation Environment.* 2004. **699**: p. 614-622.
5. King, J.C. and M.S. El-Genk, *Submersion criticality safety of fast spectrum space reactors: Potential spectral shift absorbers.* Nuclear Engineering and Design, 2006. **236**(3): p. 238-254.
6. Wheeler, A.R. and A.C. Klein, *Modeling and Analysis of a Heat Transport Transient Test Facility for Space Nuclear Systems.* Nuclear Technology, 2014. **188**(1): p. 45-62.
7. Bushman, A., et al., *The Martian Surface Reactor: An advanced nuclear power station for manned extraterrestrial exploration*, 2004, MIT-NSATR-003, Cambridge.
8. Ran, X., et al., *Safety Characteristic Analysis of Advanced Space Fast Rector (In Chinese).* Atomic Energy Scince and Technology, 2006. **4**(6).
9. Waltar, A.E. and A.B. Reynolds, *Fast Breeder Reactors*. 1981, New York: Pergamon Press. xxvi, 853 p.
10. Yuan, H. and D. Hu, *High-Order End Floating Method-for Solving Point Reactor Neutron Kinetics Equations (In Chinese).* Nuclear Power Engineering, 1993. **14**(2): p. 122-128.
11. Wulff, W. *Lumped-Parameter Models forTransient Conduction in Nuclear Reactor Components*. in *U.S. Nuclear Regulatory Commission*. 1980. Brookhaven National Lab., Upton, NY (USA).
12. Cao, Y. and A. Faghri, *A Numerical Analysis of High-Temperature Heat Pipe Startup from the Frozen State.* Journal of heat transfer, 1993. **115**(1): p. 247-254.
13. Ochterbeck, J., *Modeling of Room-Temperature Heat Pipe Startup from the Frozen State.* Journal of thermophysics and heat transfer, 1997. **11**(2): p. 165-172.
14. Zuo, Z. and A. Faghri, *A Network Thermodynamic Analysis of the Heat Pipe.* International Journal of Heat and Mass Transfer, 1998. **41**(11): p. 1473-1484.
15. Tournier, J.-M. *An Analytical Model for Liquid-Anode and Vapor-Anode AMTEC Converters*. in *Space technology and applications international forum (STAIF-97)*. 1997. AIP Publishing.
16. El-Genk, M.S. and J.-M. Tournier, *"SAIRS"-Scalable Amtec Integrated Reactor space power System.* Progress in nuclear energy (New series), 2004. **45**(1): p. 25 - 69.
17. Yuan Yuan, S.J., *Transient Analysis of Heat Pipe Cooled Space REactor Power System*, X.J. University, Editor 2014.